

Dynamics of Nanoscale Polarization Fluctuations in a Uniaxial Relaxor

P. Ondrejko¹, M. Kempa¹, J. Kulda², B. Frick², M. Appel², J. Combet², J. Dec³, T. Lukasiewicz⁴, and J. Hlinka^{1*}

¹*Institute of Physics, Academy of Sciences of the Czech Republic, Na Slovance 2, 18221 Praha 8, Czech Republic*

²*Institut Laue-Langevin, BP 156, 38042 Grenoble Cedex 9, France*

³*Institute of Materials Science, University of Silesia, Bankowa 12, PL-40-007 Katowice, Poland*

⁴*Institute of Electronic Materials Technology, 133 Wolczynska Street, 01-919 Warsaw, Poland*

(Received 16 June 2014; revised manuscript received 6 August 2014; published 16 October 2014)

We have studied neutron diffuse scattering in a $\text{Sr}_{0.61}\text{Ba}_{0.39}\text{Nb}_2\text{O}_6$ single crystal by neutron back-scattering at sub- μeV energy resolution. We can identify two response components with transverse polarization: an elastic (resolution limited) central peak, which monotonically increases with decreasing temperature, and a quasielastic central peak, having a maximum intensity around the ferroelectric phase transition close to 350 K. In contrast to previous neutron experiments on this and other relaxor materials, we were able to observe a temperature dependence of the characteristic frequency of these fluctuations, obeying the same Vogel-Fulcher law as the dynamic part of the dielectric permittivity of this material. In this way our findings provide a first direct link between the Vogel-Fulcher-type frequency dependence of dielectric permittivity and dynamic nanoscale lattice modulations with a transverse correlation length of about 5–10 unit cells.

DOI: 10.1103/PhysRevLett.113.167601

PACS numbers: 77.80.Jk, 63.50.-x, 77.84.Ek, 78.70.Nx

One of the most remarkable properties of relaxor materials is their extraordinarily large dielectric permittivity appearing over a broad temperature interval and attaining its maximum at a temperature T_{max} , which varies linearly with the logarithm of the probing frequency $[\log \nu]$, see Fig. 1(a)]. Contrary to the usual direct proportionality between the absolute temperature and the $\log \nu$, i.e., an Arrhenius relationship describing the slowing down of all usual thermally activated processes in nature, here at low frequencies T_{max} tends towards a finite characteristic temperature T_{VF} , which is typically hundreds of K above the absolute zero temperature. This type of dependence, which clearly contrasts with the Arrhenius law, is known from the dynamics of glass-forming liquids under the name of the Vogel-Fulcher (VF) law [1–7], and in general it indicates an exponentially broad spectrum of relaxation times and correlation lengths. In this respect, relaxor ferroelectrics belong to a broad family of disordered materials of current interest like fragile glass-forming liquids [8–11], structural glasses [12], diluted or frustrated spin glasses [13,14], superconducting vortex glasses [15], and confined [16] or protein-hydration water [17].

Although the relaxor-glass analogy has to be taken with care [18,19], it has been widely accepted that the VF behavior in relaxor ferroelectrics is related to a temperature-dependent length scale of nanorange polar inhomogeneities [4,20–22]. While there is clear experimental evidence for nanoscale polar entities in the low-temperature relaxor state from neutron and x-ray scattering investigations and from piezoresponse force scanning microscopy [23–37], the exact topology of the spatial polarization distribution is still debated [5,18,22]. As a consequence, the microscopic origins of the Vogel-Fulcher-type dynamics continue to

represent the most enigmatic aspect of the relaxor physics [4–7,18,20,21,38–40] and, as in the case of a glass transition [8,12], it calls for further investigations at multiple time and length scales.

A pronounced VF-type dielectric relaxation, considered as a hallmark of relaxor behavior, has been also found in many complex perovskites but also in tetragonal tungsten bronze crystals, such as $\text{Sr}_{0.61}\text{Ba}_{0.39}\text{Nb}_2\text{O}_6$ (SBN61) [41,42]. The tetragonal tungsten bronze relaxors are very interesting materials because they can be considered as almost ideal uniaxial relaxors [43–47], in which both the local polarization and the nanodomain (or polar cluster) boundaries can be expected to be parallel to the easy axis of the material (z axis in the following). Contrary to perovskite relaxors, no ferroelastic-ferroelectric domain walls exist there. Such a severe restriction on polarization correlations in uniaxial relaxors obviously drastically simplifies any considerations about the origin of their dielectric relaxation and so they are playing an attractive role of model systems for understanding the essence of relaxor behavior by itself.

A schematic representation of the nanodomain structure in tetragonal tungsten bronze-type crystals as deduced from piezoresponse force scanning microscopy measurements [30,48] is sketched in Fig. 1(c). Nanoscale domains with opposite polarization orientations are extended along the z axis and exhibit irregular boundaries within the xy plane [49,50]. This highly anisotropic picture is confirmed in diffraction experiments by disk-shaped transverse diffuse scattering intensity distributions located close to the Brillouin zone centers with nonzero L index [cf. Fig. 1(d)].

Detailed neutron scattering studies revealed that this diffuse scattering actually consists of two contributions

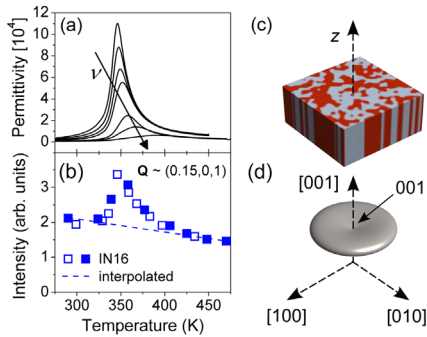


FIG. 1 (color online). Temperature dependence of (a) the real z -axis dielectric permittivity at frequencies 0.01 Hz (present work), 1 Hz, 1 kHz, 100 kHz (Ref. [42]), 1, 10, and 100 MHz (Ref. [41]); and of (b) the zero-energy-transfer scattering intensity, measured at $\mathbf{Q} \approx (0.15, 0, 1)$ in static (open squares) and dynamic (solid squares) modes of the IN16 spectrometer. Dashed line shows the interpolated scattering intensity of the DW component. Sketches (c) and (d) indicate a typical nanodomain structure of a uniaxial relaxor and the equi-intensity surface of the associated diffuse scattering.

with a distinct temperature dependence and with a distinct shape in the momentum space [51–53]. It was found that the intensity profile of the narrower component, monotonically increasing with decreasing temperature, can be well described by a simple model for scattering by domain walls and that its presence can be effectively suppressed by a bias electric field of a few kV/cm [51,53,54]. On the other hand, the intensity of the broader component has a temperature dependence similar to the dielectric permittivity with a maximum near T_{\max} and the electric field has a much smaller influence here. Accordingly, the two components have been assigned to scattering due to static domain walls (DW) and due to the order parameter fluctuations (OPF), respectively [51–53]. Both the DW and the OPF components have been reported as elastic within the resolution limits of the corresponding neutron three-axis spectrometer experiments, which only means that such scattering is due to lattice modulations that are either static or fluctuating at frequencies lower than about 100 GHz, without a possibility of making any statement about their behavior in the GHz/MHz range of the dielectric spectroscopy frequencies.

Our principal aim in the present study is to bridge the gap between the available neutron scattering and dielectric spectroscopy results by exploring the diffuse neutron scattering response at a sub-GHz energy resolution, matching the characteristic frequencies of the relaxation modes observed by dielectric spectroscopy. Taking a lesson from former attempts based on the neutron spin-echo technique [37,55] and producing results dominated by the signal of a strong central peak, elastic even on the sub-GHz scale, we have opted for the neutron backscattering technique, which is capable of detecting quasielastic scattering at the foot of an elastic line having several orders of magnitude higher intensity. With this approach the quasielastic character of

the OPF component is clearly revealed with a time scale matching the strongly temperature dependent Cole-Cole band present in the high-frequency dielectric measurements [41]. In this way, our results provide a first direct link between dynamic nanoscale lattice modulations and the dielectric relaxation modes with their Vogel-Fulcher-type frequency dependence.

Our neutron scattering experiments were performed using the backscattering spectrometers at the ILL Grenoble (France) on a cylindrical SBN61 single crystal grown by the Czochralski method and having a volume of about 3 cm³ [42]. Most parts of the measurements were carried out using the standard configuration of the “old” IN16 [an unpolished Si(111) Doppler monochromator, unpolished Si(111) analyzers] providing instrumental energy resolution of 0.8 μeV (200 MHz) at scattered neutron wave vector of $k_f = 1 \text{ \AA}^{-1}$ and operating with a dynamic range of $\pm 4 \mu\text{eV}$. The sample was mounted in a standard cryofurnace with its $(h0l)$ plane horizontal and the measurements were carried out at momentum transfers close to the 001 Brillouin zone center, imposed by the $k_f = 1 \text{ \AA}^{-1}$. Some data have also been taken while testing the newly commissioned IN16B backscattering spectrometer, operating in a similar configuration as IN16 with an energy resolution of 1 μeV . Here we were able to draw benefits from the increased flexibility of the new instrument, permitting us to carry out directly momentum transfer and temperature scans at a given energy transfer window [56]. In our case data were taken at energy transfers of 0, 3, and 8 μeV .

The present measurements of the diffuse scattering have been carried out at the $\mathbf{Q} \approx (0.15, 0, 1)$ momentum transfer in the 290–470 K temperature range. The temperature dependence of the scattering intensity at zero energy transfer is shown in Fig. 1(b). The pronounced broad maximum near the transition temperature [57] $T_C = 346 \text{ K}$, with a shape similar to that of the temperature dependence of dielectric permittivity [see Fig. 1(a)], testifies that the diffuse scattering intensity detected in our experiment contains a significant contribution of the OPF diffuse scattering component. Moreover, since the temperature dependence shown in Fig. 1(b) is qualitatively similar to the three-axis spectrometer measurements at $\mathbf{Q} \approx (0.1, 0.1, 2)$ shown in Fig. 2 of Ref. [52], we can infer that both DW and OPF components are considerably contributing to the zero-energy-transfer intensity in the present experiment.

Although the detected diffuse scattering intensity falls down rapidly with the increasing energy transfer, the high counting statistics allowed us to trace and analyze the intensity decay up to a few μeV . Selected spectra are depicted in Figs. 2(a)–2(e).

The 290 K temperature is well below the transition range, so that the OPF component is negligible there and in fact, the entire 290 K spectrum can be well adjusted to a pseudo-Voigt function with full width at half maximum of 0.77 μeV , superposed on a constant background. This full width at half maximum matches the nominal energy

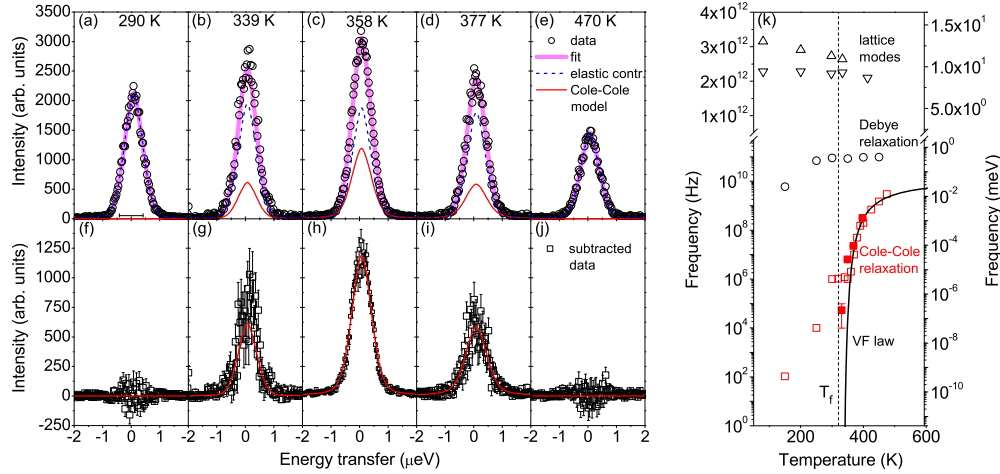


FIG. 2 (color online). Left: Inelastic neutron scattering spectra at $\mathbf{Q} \approx (0.15, 0, 1)$ (point symbols), fitted to the model defined in Eqs. (1)–(3) (thick solid lines). Dashed lines refer to the resolution-limited DW contribution of Eq. (1), thin solid lines show the OPF contribution [Eqs. (2)–(3)]. Lower panels (f)–(j) show the OPF part of the signal obtained by subtraction of the DW contribution from the original spectra. Right: Temperature dependence of polar mode frequencies from z -axis dielectric spectra. Triangles stand for the lowest-frequency polar phonon frequencies [58], open circles and squares for the relaxation frequencies of Debye and Cole-Cole modes [41]. Solid line indicates the VF-type temperature dependence of Cole-Cole mode frequency ν_0 with parameters of Ref. [41,59]. Full squares stand for the Cole-Cole mode frequency ν_0 as determined from the fits shown in panels (a)–(j).

resolution of the instrument, which corroborates the anticipations that the DW component is essentially static. Therefore, this pseudo-Voigt function was adopted here as an energy resolution function $f_{\text{RL}}(\nu)$.

Other spectra were analyzed by three different methods. First of all, we noticed that spectra taken at temperatures around 350 K did not give a nice fit to this $f_{\text{RL}}(\nu)$. Obviously, it suggests the presence of the anticipated inelastic OPF component. Since the previous studies have demonstrated that the intensity of the DW contribution shows a weak, monotonic decrease with temperature, we have assumed here that the $\nu = 0$ intensity of the DW contribution $I_{\text{DW}}(0, T)$ has a simple linear temperature dependence that can be estimated by interpolation between 270 and 470 K zero-energy-transfer measurements [dashed line in Fig. 1(b)]. Then, the intensity of the scattering by the DW component can be estimated by

$$I_{\text{DW}}(\nu, T) = I_{\text{DW}}(0, T) \frac{f_{\text{RL}}(\nu)}{f_{\text{RL}}(0)}. \quad (1)$$

This contribution, shown by dashed lines in Figs. 2(a)–2(e), was subtracted from the measured spectra. The resulting spectra, shown in Figs. 2(f)–2(j), have been then fitted to a simple model of fluctuating polarization in the form

$$I(\nu) = K n_{\text{BE}}(\nu) \chi''(\nu) \otimes f_{\text{RL}}(\nu) + f_b, \quad (2)$$

where $K > 0$, f_b are a frequency- and temperature-independent scaling factor and constant background, respectively, n_{BE} is the Bose-Einstein factor, and χ'' is the imaginary part of a dynamical susceptibility described by a Cole-Cole model [41,60,61]

$$\chi^*(\nu) = \chi'(\nu) - i\chi''(\nu) = \frac{\Delta\chi}{1 + (i\nu/\nu_0)^{1-\alpha}} + \chi_\infty. \quad (3)$$

with $\chi_\infty = 0$, where ν_0 stands for the average relaxation frequency, α is a characteristic shape index varying between 0 and 1, and $\Delta\chi$ has (in the case of the dielectric response) the meaning of a dielectric strength. For $\alpha = 0$, this model reduces to the usual Debye model, describing a system with a single exponential decay, while the nonzero α allows us to describe systems with a range of relaxation times.

Moreover, when we have taken the α values of the Cole-Cole relaxation observed from the SBN61 dielectric study of Ref. [41] and fitted this model to the spectra of Figs. 2(f)–2(j), the resulting ν_0 frequencies corresponded well with those determined from dielectric measurements [see Fig. 2(k)].

Second, being encouraged by these findings, we have analyzed more closely the high-energy tails of the original spectra of Figs. 2(a)–2(e). In order to reduce the spread of the data points, the measured spectra were numerically smoothed with a $0.8 \mu\text{eV}$ wide sliding window. Examples of such smoothed spectra are shown in Fig. 3. At energies above $1.5 \mu\text{eV}$, the DW contribution to the measured signal is negligible and all the intensity exceeding the constant inelastic background can be ascribed to the inelastic scattering due to the OPF component. First of all, the data shown in Fig. 3 directly reveal that the OPF component of the 406 K spectrum is noticeably broader than that of the 358 K spectrum. The temperature dependence of the characteristic frequency of the OPF component can be more greatly appreciated when the scattering intensity at a fixed energy transfer is traced as a function of temperature.

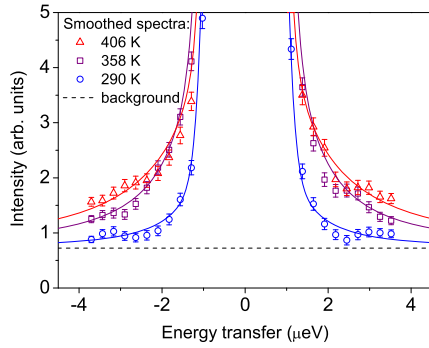


FIG. 3 (color online). Inelastic neutron scattering spectra at $\mathbf{Q} \approx (0.15, 0, 1)$, smoothed with a $0.8 \mu\text{eV}$ wide sliding window. Solid lines are calculated spectra from the model defined by Eqs. (1)–(3) with values of α , ν_0 , and $\Delta\chi$ taken from the analysis [41] of dielectric data by means of the Cole-Cole model.

Such plots are shown in Fig. 4(a). With the increasing energy transfer, the peak position is shifting towards higher temperatures, and this shift actually follows quite well the Vogel-Fulcher law determined from the dielectric measurements [41].

Third, we have compared the neutron spectra directly with the dielectric data. As a matter of fact, Ref. [41] suggests that there are two polar excitations in the SBN crystals with relaxation frequencies below the phonon frequency range [see Fig. 2(k)]. One of them is a Debye-type relaxation mode with frequency in the range of 100 GHz, the other is a strongly temperature-dependent Cole-Cole relaxation band in the MHz-GHz range. In order to make the correspondence of the OPF scattering with the Cole-Cole dielectric relaxation even more apparent, we have directly calculated the diffuse scattering intensity from the model of Eqs. (1)–(3) with parameter values of α , ν_0 , and $\Delta\chi$ taken strictly as those of the Cole-Cole mode [59] of the dielectric spectra of Ref. [41]. Results of these calculations, shown as solid lines in Fig. 3 and also as data points in Fig. 4(b), are in a fairly good agreement with the neutron scattering data. We can thus conclude that within the experimental precision, there is essentially no difference in the Cole-Cole mode frequency determined from dielectric and neutron scattering data. The absence of wave vector dependence of the Cole-Cole mode frequency may indicate that the OPF excitations do not have well-defined wave vectors.

These three different approaches all testify that the OPF diffuse scattering component in SBN61 is caused by the same polar fluctuations that are responsible for Vogel-Fulcher-type dielectric relaxation. At the same time, the Lorentzian profile of the OPF diffuse scattering component within the a^*b^* reciprocal plane has been thoroughly studied in the past and its 5–10 unit cell transverse correlation length is well established [51–53]. Therefore, the present results allow us to combine the information about temporal and spatial correlations associated with Vogel-Fulcher-type dielectric relaxations of SBN61.

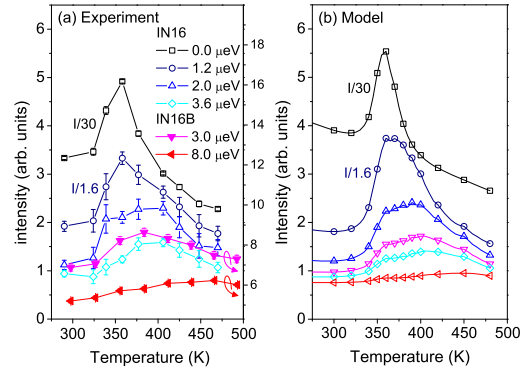


FIG. 4 (color online). Temperature dependence of the scattering intensity obtained (a) from experimental spectra measured on IN16 and fixed-window measurements on IN16B at $\mathbf{Q} \approx (0.15, 0, 1)$ and (b) from the same model as in Fig. 3. Both the experimental and model spectra were smoothed as in Fig. 3.

Let us stress that coexistence of quasistatic and quasi-elastic neutron diffuse scattering has been also demonstrated in triaxial relaxor $\text{Pb}(\text{Mg}_{1/3}\text{Nb}_{2/3})\text{O}_3$ (PMN) [37]. In particular, the dynamic component falling in the 10–100 GHz range window of the neutron spin-echo instrument [37] seems to be analogous to the OPF component of SBN61. Unfortunately, the neutron scattering data of PMN were only analyzed assuming a single-exponential decay and a simple Arrhenius temperature dependence, even though the dielectric response of PMN is known to show a clear VF law and very broad range of relaxation times [4,20,21,39]. Moreover, the ferroelectric soft mode of triaxial relaxors is overdamped [62] near T_{max} and so most likely the soft mode also contributes to the observed quasielastic diffuse scattering [24,33,55,63]. In contrast, phonon frequencies of uniaxial SBN61 do not show such a pronounced softening and their contribution is well separated from relaxations associated with VF dynamics [see Fig. 2(k)].

In summary, we have exploited the possibilities of IN16 and IN16B backscattering spectrometers at ILL Grenoble which have about 2–3 orders of magnitude better resolution than the cold neutron three-axis spectrometers. By this technique, we have been able to probe excitations in the GHz and sub-GHz frequency range and to confirm explicitly the earlier conjecture about the dynamic nature of the Lorentzian component of transverse diffuse scattering of SBN61. We could clearly demonstrate that associated inelastic spectra are fully consistent with the temperature- and frequency-dependent susceptibility of the Cole-Cole relaxation band as derived from dielectric studies. Therefore, these measurements provide the missing link that allows us to relate directly the correlation lengths of the OPF diffuse scattering with the polarization fluctuations responsible for the Vogel-Fulcher-type dielectric behavior of uniaxial relaxors.

This work was supported by the Ministry of Education, Youth and Sports of the Czech Republic (Project No. LG14037).

- *Corresponding author.
hlinka@fzu.cz
- [1] M. Cyrot, *Phys. Lett.* **83A**, 275 (1981).
- [2] H. Vogel, *Phys. Z.* **22**, 645 (1921).
- [3] G. S. Fulcher, *J. Am. Ceram. Soc.* **8**, 339 (1925).
- [4] R. Blinc, *Advanced Ferroelectricity* (Oxford University Press, New York, 2011).
- [5] R. Pirc and R. Blinc, *Phys. Rev. B* **76**, 020101(R) (2007).
- [6] A. E. Glazounov and A. K. Tagantsev, *Appl. Phys. Lett.* **73**, 856 (1998).
- [7] D. Viehland, S. J. Jang, L. E. Cross, and M. Wuttig, *J. Appl. Phys.* **68**, 2916 (1990).
- [8] P. G. Debenedetti and F. H. Stillinger, *Nature (London)* **410**, 259 (2001).
- [9] P. K. Dixon, L. Wu, S. R. Nagel, B. D. Williams, and J. P. Carini, *Phys. Rev. Lett.* **65**, 1108 (1990).
- [10] S. Whitelam, L. Berthier, and J. P. Garrahan, *Phys. Rev. Lett.* **92**, 185705 (2004).
- [11] P. Lunkenheimer, A. Pimenov, M. Dressel, Yu. G. Goncharov, R. Böhmer, and A. Loidl, *Phys. Rev. Lett.* **77**, 318 (1996).
- [12] E. Courtens, *Phys. Rev. Lett.* **52**, 69 (1984).
- [13] J. L. Tholence, *Solid State Commun.* **35**, 113 (1980).
- [14] S. Shtrikman and E. P. Wohlfarth, *Phys. Lett.* **85A**, 467 (1981).
- [15] C. Reichhardt, A. van Otterlo, and G. T. Zimányi, *Phys. Rev. Lett.* **84**, 1994 (2000).
- [16] L. Liu, S.-H. Chen, A. Faraone, C.-W. Yen, and C.-Y. Mou, *Phys. Rev. Lett.* **95**, 117802 (2005).
- [17] S.-H. Chen, L. Liu, E. Fratini, P. Baglioni, A. Faraone, and E. Mamontov, *Proc. Natl. Acad. Sci. U.S.A.* **103**, 9012 (2006).
- [18] A. K. Tagantsev, *Phys. Rev. Lett.* **72**, 1100 (1994).
- [19] D. Nuzhnyy, J. Petzelt, M. Savinov, T. Ostapchuk, V. Bovtun, M. Kempa, J. Hlinka, V. Buscaglia, M. T. Buscaglia, and P. Nanni, *Phys. Rev. B* **86**, 014106 (2012).
- [20] L. E. Cross, *Ferroelectrics* **76**, 241 (1987).
- [21] G. A. Samara, *J. Phys. Condens. Matter* **15**, R367 (2003).
- [22] J. Hlinka, *J. Adv. Dielect.* **02**, 1241006 (2012).
- [23] V. V. Shvartsman, B. Dkhil, and A. L. Kholkin, *Annu. Rev. Mater. Res.* **43**, 423 (2013).
- [24] J. Hlinka, S. Kamba, J. Petzelt, J. Kulda, C. A. Randall, and S. J. Zhang, *J. Phys. Condens. Matter* **15**, 4249 (2003).
- [25] I. K. Bdikin, J. A. Prez, I. Coondoo, A. M. R. Senos, P. Q. Mantas, and A. L. Kholkin, *J. Appl. Phys.* **110**, 052003 (2011).
- [26] G. Xu, Z. Zhong, Y. Bing, Z.-G. Ye, and G. Shirane, *Nat. Mater.* **5**, 134 (2006).
- [27] P. Bonneau, P. Garnier, and G. Calvarin, *J. Solid State Chem.* **91**, 350 (1991).
- [28] V. V. Shvartsman and A. L. Kholkin, *J. Appl. Phys.* **101**, 064108 (2007).
- [29] H. You and Q. M. Zhang, *Phys. Rev. Lett.* **79**, 3950 (1997).
- [30] V. V. Shvartsman, W. Kleemann, T. Lukasiewicz, and J. Dec, *Phys. Rev. B* **77**, 054105 (2008).
- [31] K. Hirota, Z.-G. Ye, S. B. Wakimoto, P. M. Gehring, and G. Shirane, *Phys. Rev. B* **65**, 104105 (2002).
- [32] M. Matsuura, H. Endo, M. Matsushita, Y. Tachi, Y. Iwasaki, and K. Hirota, *J. Phys. Soc. Jpn.* **79**, 033601 (2010).
- [33] P. M. Gehring, H. Hiraka, C. Stock, S.-H. Lee, W. Chen, Z.-G. Ye, S. B. Vakhrušev, and Z. Chowdhuri, *Phys. Rev. B* **79**, 224109 (2009).
- [34] L. Xie, Y. L. Li, R. Yu, Z. Y. Cheng, X. Y. Wei, X. Yao, C. L. Jia, K. Urban, A. A. Bokov, Z.-G. Ye, and J. Zhu, *Phys. Rev. B* **85**, 014118 (2012).
- [35] J. Dec, W. Kleemann, V. V. Shvartsman, D. C. Lupascu, and T. Lukasiewicz, *Appl. Phys. Lett.* **100**, 052903 (2012).
- [36] M. Pasciak, T. R. Welberry, J. Kulda, M. Kempa, and J. Hlinka, *Phys. Rev. B* **85**, 224109 (2012).
- [37] C. Stock, L. Van Eijck, P. Fouquet, M. Maccarini, P. M. Gehring, G. Xu, H. Luo, X. Zhao, J.-F. Li, and D. Viehland, *Phys. Rev. B* **81**, 144127 (2010).
- [38] D. Viehland, M. Wuttig, and L. E. Cross, *Ferroelectrics* **120**, 71 (1991).
- [39] V. Bovtun, S. Kamba, A. Pashkin, M. Savinov, P. Samoukhina, J. Petzelt, I. P. Bykov, and M. D. Glinchuk, *Ferroelectrics* **298**, 23 (2004).
- [40] V. Westphal, W. Kleemann, and M. D. Glinchuk, *Phys. Rev. Lett.* **68**, 847 (1992).
- [41] E. Buixaderas, M. Savinov, M. Kempa, S. Veljko, S. Kamba, J. Petzelt, R. Pankrath, and S. Kapphan, *J. Phys. Condens. Matter* **17**, 653 (2005).
- [42] T. Lukasiewicz, M. A. Swirkowicz, J. Dec, W. Hofman, and W. Szyrski, *J. Cryst. Growth* **310**, 1464 (2008).
- [43] W. Kleemann, J. Dec, V. V. Shvartsman, Z. Kutnjak, and T. Braun, *Phys. Rev. Lett.* **97**, 065702 (2006).
- [44] R. R. Neurgaonkar, J. R. Oliver, W. K. Cory, L. E. Cross, and D. Viehland, *Ferroelectrics* **160**, 265 (1994).
- [45] V. V. Shvartsman and D. C. Lupascu, *J. Am. Ceram. Soc.* **95**, 1 (2012).
- [46] W. Kleemann, *J. Phys. Condens. Matter* **18**, L523 (2006).
- [47] F. M. Jiang, J.-H. Ko, and S. Kojima, *Phys. Rev. B* **66**, 184301 (2002).
- [48] V. Ya. Shur, V. A. Shikhova, A. V. Ievlev, P. S. Zelenovskiy, M. M. Neradovskiy, D. V. Pelegov, and L. I. Ivleva, *J. Appl. Phys.* **112**, 064117 (2012).
- [49] G. Fogarty, B. Steiner, M. Cronin-Golomb, U. Laor, M. H. Garrett, J. Martin, and R. Uhrin, *J. Opt. Soc. Am. B* **13**, 2636 (1996).
- [50] N. R. Ivanov, T. R. Volk, L. I. Ivleva, S. P. Chumakova, A. V. Ginzberg, *Crystallogr. Rep. (Transl. Kristallografiya)* **47**, 1023 (2002).
- [51] F. Prokert and R. Schalge, *Phys. Status Solidi B* **87**, 179 (1978).
- [52] S. A. Borisov, N. M. Okuneva, S. B. Vakhrušev, A. A. Naberezhnov, T. R. Volk, and A. V. Filimonov, *Phys. Solid State* **55**, 334 (2013).
- [53] S. N. Gvasaliya, R. A. Cowley, L. I. Ivleva, S. G. Lushnikov, B. Roessli, and A. Zheludev, *J. Phys. Condens. Matter* **26**, 185901 (2014).
- [54] R. A. Cowley, J. D. Axe, and M. Iizumi, *Phys. Rev. Lett.* **36**, 806 (1976).
- [55] S. Vakhrušev, A. Ivanov, and J. Kulda, *Phys. Chem. Chem. Phys.* **7**, 2340 (2005).
- [56] B. Frick, J. Combet, and L. van Eijck, *Nucl. Instrum. Methods Phys. Res., Sect. A* **669**, 7 (2012).
- [57] R. Paszkowski, K. Wokulska, T. Lukasiewicz, and J. Dec, *Cryst. Res. Technol.* **48**, 413 (2013).
- [58] R. E. Wilde, *J. Raman Spectrosc.* **22**, 321 (1991).
- [59] Vogel-Fulcher law parameters determined in Ref. [41] are $\nu_\infty = 14.0 \times 10^9$ Hz, $E_0/k = 270$ K, and $T_{VF} = 330$ K.
- [60] K. S. Cole and R. H. Cole, *J. Chem. Phys.* **9**, 341 (1941).
- [61] A. K. Jonscher, *Dielectric Relaxation in Solids* (Chelsea Diel Press, London, 1983).
- [62] A. Al-Zein, J. Hlinka, J. Rouquette, and B. Hehlen, *Phys. Rev. Lett.* **105**, 017601 (2010).
- [63] H. Hiraka, S.-H. Lee, P. M. Gehring, G. Xu, and G. Shirane, *Phys. Rev. B* **70**, 184105 (2004).